



OPEN

Examining the physico-chemical, structural and thermo-mechanical properties of naturally occurring *Acacia pennata* fibres treated with KMnO_4

K. R. Jaya Sheeba¹, Retnam Krishna Priya^{1✉}, Krishna Prakash Arunachalam², S. Shobana³, Siva Avudaiappan^{4,5,6✉} & Erick Saavedra Flores⁷

Natural fiber is a viable and possible option when looking for a material with high specific strength and high specific modulus that is lightweight, affordable, biodegradable, recyclable, and eco-friendly to reinforce polymer composites. There are many methods in which natural fibres can be incorporated into composite materials. The purpose of this research was to evaluate the physico-chemical, structural, thermal, and mechanical properties of *Acacia pennata* fibres (APFs). Scanning electron microscopy was used to determine the AP fibers' diameter and surface shape. The crystallinity index (64.47%) was discovered by XRD. The irregular arrangement and rough surface are seen in SEM photos. The findings demonstrated that fiber has high levels of cellulose (55.4%), hemicellulose (13.3%), and low levels of lignin (17.75%), which were determined through chemical analysis and validated by Fourier Transform Infrared Spectroscopy (FTIR). By using FTIR, the functional groups of the isolated AP fibers were examined, and TG analysis was used to look into the thermal degrading behaviour of the fibers treated with potassium permanganate (KMnO_4). Due to their low density (520 kg/m^3) and high cellulose content (55.4%), they have excellent bonding qualities. Additionally, tensile tests were used for mechanical characterisation to assess their tensile strength (685 MPa) and elongation.

Our living planet Earth is the source of abundant wealth and resources. It provides shelter for over seven million species of plants and animals. Today's diverse cellulose fibers, which have evolved over the past few decades and include flax, hemp, sisal, cotton, kenaf, jute, bamboo, coconut, and date palm, provide a variety of advantages over synthetic fibers (mostly glass, carbon, and plastic) due to their renewable nature^{1,2}. A number of natural fiber materials can be distinguished by their place of origin in nature. According to specific classifications made by researchers³⁻⁸ these materials fall into three categories: fibers produced from animals, minerals, and plants. These fibers are used in a variety of composite material manufacturing processes⁹⁻¹³. In comparison to standard reinforcing materials, natural fibres have greater thermal and acoustic insulating qualities, an acceptable specific strength, cheap cost, and low density¹⁴⁻¹⁸. The maturity and origin of the plant, as well as the methods and techniques used to extract the fiber from the stem, still affect the mechanical properties of the fibers¹⁹. For every good alternative material without sacrificing the mechanical properties of the fiber, these are some better fiber-yielding plants that are reasonably priced. *Acacia pennata* (AC) is one such plant, and it is most readily available in tropical

¹PG & Research Department of Physics, Holy Cross College (Autonomous), Nagercoil, Affiliated to Manonmanium Sundaranar University, Tirunelveli, Tamil Nadu 629004, India. ²Department of Civil Engineering, University College of Engineering Nagercoil, Anna University, Nagercoil 629004, India. ³Green Technology and Sustainable Development in Construction Research Group, Van Lang School of Engineering and Technology, Van Lang University, Ho Chi Minh City, Viet Nam. ⁴Departamento de Ingeniería Civil, Universidad de Concepción, 4070386 Concepción, Chile. ⁵Centro Nacional de Excelencia Para la Industria de la Madera (CENAMAD), Pontificia Universidad Católica de Chile, Av. Vicuña Mackenna 4860, 8331150 Santiago, Chile. ⁶Department of Physiology, Saveetha Dental College and Hospitals, SIMATS, Chennai 600077, India. ⁷Departamento de Ingeniería en Obras Civiles, Universidad de Santiago de Chile, Av. Ecuador 3659, Estación Central, Santiago, Chile. ✉email: krishnapriya@holycrossngl.edu.in; savudaiappan@udec.cl

areas of India. In contrast, natural fibers were safe, renewable, biodegradable, eco-friendly, and affordable with high specific strength^{20,21}. Ripples of applications are found in natural fibers from household little equipment's to aviation. It is because of the efficient properties possessed by these natural composites like light weight, high aspect ratio, low density, soundproof, good thermal and mechanical properties, biodegradability etc.

According to the literature review, natural fibers will become more significant in the future since they are readily available, recyclable, and environmentally friendly²². For automotive applications, polymer composites with various fillers and / or reinforcements are often employed. In order to ensure that the overall cost of the vehicle is lower and that the automobile manufacturing process is more sustainable, numerous such composites have recently been created for use in interior and exterior sections of cars^{23,24}. The usefulness of a fiber for commercial purposes is decided by features such as length, strength, pliability, elasticity, abrasion resistance, flexibility, etc., aside from economic considerations. Younger fibers from plants tend to be stronger and more elastic than the older ones^{25,26}. The cellulose is the main content of fibers which corresponds to the crystalline nature of the fibers and the presence of hemicellulose, pectin, lignin should be wiped or reduced by processing for improvements. Also, the antibacterial property is a noted one. Animal, mineral, and plant fibers are specifically the three groups into which natural fibers fall²⁷. The utilisation of natural fibres for the purpose of filling and reinforcing thermoplastic polymers is currently the most prevalent method of reinforcement in today's world. Tensile strength is the most crucial mechanical characteristic of natural fibers that makes them ideal for creating composite materials. Most naturally occurring fibers fall short in the hydrophilic department, which results in poor chemical resistance, subpar mechanical qualities, and porous structures that restrict the engineering uses of these materials^{28,29}. When choosing a specific fibre to be utilised in a composite material or in any other industrial application, the density, young's modulus, elongation, and stiffness are other crucial parameters that must be taken into account^{30–32}. Natural fibres make excellent insulation against heat, sound, and electricity. They are also easily burnable and biodegradable³³. For instance, composites have been utilised in bumpers, roofs, doors, panels, seats of cars, buses, and other vehicles in the automotive sector. Researchers are now interested in improving mechanical qualities like compression, tensile, flexural, or impact strength, as well as wear behaviour, which represent the great achievement of good materials³⁴. Particularly, composite materials are being created and modified in an effort to enhance existing products as well as to offer new ones in a sustainable and ethical manner³⁵.

The goal of the current study is to examine and compare the physical, chemical, thermal, mechanical, and morphological analysis of *Acacia pennata* fibers (APFs) with that of other probable natural fibres mentioned in the literature. In order to determine the APFs bonding properties, the surface roughness of the material was also measured using a three-dimensional non-contact surface roughness tester. To determine the contents of cellulose, hemicellulose, lignin, pectin, wax, moisture, and ash, a chemical analysis was carried out. In addition, thermogravimetric analysis, X-ray diffraction (XRD), and Fourier transform infrared (FTIR) examinations were used to analyse the crystalline phases and compounds.

Materials and methods

Materials

The *Acacia pennata* fiber was treated using distilled water, NaOH pellets, and a potassium permanganate pellets in acetone. This was acquired from Premier Chemicals in Nagercoil, Kanniyakumari district, Tamil Nadu, India.

Extraction method of *Acacia pennata* fiber from the plant

Acacia pennata is a large scrambling or climbing shrub. It can grow up to a height of almost 100 m. Its trunk and branches are prickly and smooth. The stem of *Acacia pennata* fibers were gathered from Tamilnadu-Kerala border (near Panachamoodu and Vellarada area). The fiber has been separated from its bark of the plant and then allowed to dry at ambient temperature (27 °C) for few days. The dried fibers are treated with distilled water for about 20 min for microbial degradation before treating the fiber with alkali (NaOH). The dried fiber sections were pre-treated with NaOH aqueous solution and the potassium permanganate (KMnO₄) solution was prepared with the help of acetone and KMnO₄ pellets. The importance of this treatment for improving surface properties was also addressed in depth. This allowed us to reduce the hydrophilic capacity and increase the adhesion between the fibers and polymers³⁶. The fibers were soaked in this (0.1 M NaOH) solution for 20 min. The fibers were removed after 20 min and dried for 10 to 15 days at room temperature (27 °C). After drying, the fiber sections are immersed in KMnO₄ solution for about 15 minutes³⁷. Then, these fibers were allowed to dry at ambient temperature. The dried AP fibers were chopped into powder form or broken into little fiber strips based on the need of analysis. KMnO₄ treated AP fibers were packed in zip-lock cover and store in room temperature. Figure 1 shows the pictures of *Acacia pennata* plant fiber and its chemical treatments.

Experimental techniques

Powder XRD technique

Powder X-ray diffraction (PXRD) is a method for determining if a material is crystalline or amorphous³⁸. It is a quick analytical method that can reveal the size of unit cells and is mostly used to determine a crystalline material's phase. Copper (Cu) is the most common target material for powder x ray diffraction, and the powder sample were subjected to X-ray diffraction using CuK α (i.e., CuK α is the emission of copper) radiation with a wavelength of 1.5406 nm in a Bruker x-ray diffractometer. A 2 θ range X-ray diffraction examination was performed with angles ranging from 3° to 70°. In the spectrum of the APFs, the integrated intensities of the Bragg peaks were recognised, and their crystallinity indices were calculated. The crystallinity index (CI) of the natural fiber was measured using the traditional peak height technique developed by Segal et al³⁹.

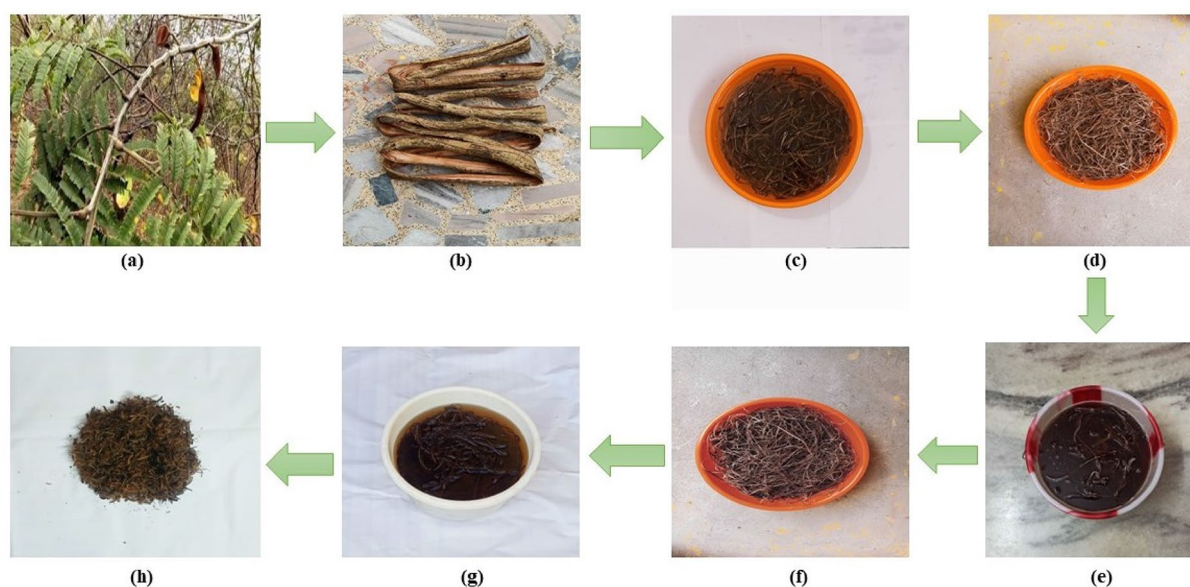


Figure 1. Images of an (a) AP plant, (b) AP stem fiber, (c) water retting, (d) untreated dried AP fibers, (e) AP fibres treated with NaOH, (f) Dried NaOH treated AP fibers, (g) AP fibres treated with KMnO₄, (h) Dried KMnO₄ treated AP fibers.

$$CI = [(H_{002} - H_{am})/H_{002}] \times 100\% \quad (1)$$

where, H_{002} is the height of the crystalline peak situated around 22° and 23°; H_{am} is the height of amorphous peak situated around 14° and 16°.

The crystallite size (CS) of the natural fiber were calculated through the following equation⁴⁰;

$$CS = [0.89\lambda/\beta \cos \theta] \quad (2)$$

where, β is the full-width at half-maximum (FWHM) value of peaks; θ is the Bragg's angle⁴¹.

FTIR techniques

A crucial method for locating significant groups is Fourier-transform infrared (FTIR) spectroscopy⁴². “Perkin Elmer Spectrum Two” FTIR spectrometer with a scan rate of 32 per minute, a resolution of 2 cm⁻¹, and a wave number range between 4000 cm⁻¹ and 400 cm⁻¹ were used to obtain the FTIR spectra of the APFs.

SEM techniques

A scanning electron microscope (SEM) with EDS is used to investigate the topography and morphology of the surfaces of materials as well as biological samples. EDS is used to facilitate elemental recognition. A concentrated electron beam is used to scan a sample's surface in a scanning electron microscope (SEM), which creates images of the sample. The spatial correlations between the various matrices' and reinforcement fibers' constituent parts have been clarified by SEM studies⁴³. Using a scanning electron microscope, the surface morphology of APFs was studied (JEOL JSM-6390LV)⁴⁴⁻⁴⁶. Magnification of the JEOL JSM-6390LV is on the order of 3,00,000 × with high resolution 3.0-nm, where fine details of the specimens can be observed.

Thermo-gravimetric techniques

Thermo-gravimetric analysis by Perkin Elmer was used to access the thermal stability behaviour of APFs. The curve plots the temperature difference between the reference material and the sample material against time or temperature. The amount and rate of change in a material's weight as a function of temperature or time in an environment of nitrogen, helium, air, another gas, or in a vacuum are measured using thermo-gravimetric analysis (TG). The method can identify materials that experience weight gains or loss as a result of oxidation, dehydration, or other processes⁴⁷.

Density using pycnometer

The thickness (density) of natural fibers is frequently measured with a pycnometer⁴⁸. The fiber sample is simply dried at room temperature before use to remove moisture⁴⁹. If moisture remains in the fiber material, a vacuum desiccator can be employed to eliminate it completely. The samples are then thoroughly pulverised and placed in the pycnometer to measure the density⁵⁰. Toluene is used as an immersion solvent when measuring the densities of untreated and KMnO₄ treated AP fibres in accordance with ASTM D578-89 standard. The fibres must be soaked in toluene for at least two hours before being weighed to assess their density. Density of APF is derived from;

$$\rho_f = \frac{(m_2 - m_1)}{[(m_3 - m_1) - (m_4 - m_2)]} * \rho_t \quad (3)$$

where, m_1 —mass of dry empty pycnometer (g); m_2 —mass of pycnometer + fiber (g); m_3 —mass of pycnometer + toluene (g); m_4 —mass of pycnometer + toluene + fiber (g); ρ_t —density of toluene (0.867 g/cm³); ρ_f —density of natural fiber in g/cm³^{351–57}.

CHNS (elemental) analysis techniques

Using a CHNS analyzer, model Elementar Vario EL III Instruments based on the principle of Dumas's method⁵⁸, which involves the complete and quick oxidation of the sample by "flash combustion," one may determine the percentages of C, H, N, S, (carbon, hydrogen, nitrogen, sulphur and oxygen elements) in organic compounds. To provide carbonate and organic carbon and to get a general idea of the composition of the organic matter (i.e., to distinguish between marine and terrigenous sources, based on total organic carbon / total nitrogen [C/N] ratios), elemental analyses of total nitrogen and carbon (and sulphur) are conducted.

Tensile strength analysis

There are various reasons to undertake tensile tests. Typically, Zwick/Roell⁵⁹ specimens are used for the tensile test⁶⁰. The maximum stress that the material can withstand or the stress required to generate substantial plastic deformation are two ways to assess the strength of an object of interest. A computerised tensile testing machine was used for the tensile testing analysis. The tensile mechanical characteristics of a material are described in depth via tensile testing and also these tests were performed with ASTM-D412 international standards⁵⁹. These characteristics can be represented graphically as a stress/strain curve to display information such as the point at which the material failed and to provide information on characteristics such the elastic modulus, strain, and yield strength⁶¹. The tests are conducted at a temperature of 21 °C, a cross-head speed of 30 mm/min, and a relative humidity of 65 ± 2%⁶². To confirm the accuracy of the tensile test, 10 fibers, each 50 mm long, are tested^{63–71}. Records are kept of the average tensile strength, elongation at break, and strain rate. The following empirical relationship governs the tensile strength of the AP fibers;

$$T = \frac{F}{A} \quad (4)$$

where; F is the force in Newtons, A is cross-sectional area in mm² and T is the tensile strength in MPa^{72,73}.

Stress–strain curves are used to evaluate the mechanical characteristics of AP fibers, including their tensile strength and percentage of elongation^{70,74}. A microscope is used to conduct a comprehensive longitudinal direction of the chosen acacia pennata fibers in order to measure their average diameter. Additionally, from the SEM images, the thickness of the fibers is calculated using the ImageJ software⁵⁹. Nearly the same diameter was obtained by both techniques. The shape of APFs cross section is round^{53,75–77}. The angle formed by the helical winding orientations of cellulose microfibrils is known as the microfibril angle (MFA). A plant fibers strength and stiffness are often affected by the amount of cellulose and the spiral-shaped wink. The Global deformation equation is used to determine the microfibrillar angle (α) of AP fibers.

$$\epsilon = \ln\left(1 + \frac{\Delta L}{L_0}\right) = -\ln(\cos\alpha) \quad (5)$$

where ϵ —strain, α —micro-fibril angle (degree) and $(\Delta L/L_0)$ —ratio of elongation^{50,52–54,78,79}.

The term "Young's modulus" is used to describe a material's resistance to elastic deformation under load. It displays the strength of a material, to put it another way.

$$E = \frac{\sigma(\text{Tensile strength})}{\epsilon(\text{strain})} = \frac{\left(\frac{F}{A}\right)}{(\Delta L/L_0)} \quad (6)$$

where, F—applied force; E—young's modulus (GPa) of the fiber; A—cross-sectional area of the fiber and $\Delta L/L_0$ —ratio of elongation⁷⁴.

The elongation at break is the ratio of the modified length to the original length when a test specimen is fractured. It demonstrates how naturally occurring plant fiber may withstand changes without breaking. It is possible to calculate the elongation at break of the AP fiber in accordance with ISO/IEC 17,025^{80,81} tensile test.

Chemical analysis test

Chemical analysis tests were used to identify the chemical composition of natural fibers and how it affected their mechanical qualities. To study the percentages of chemical compositions (cellulose, hemicelluloses, lignin, pectin, wax, and ash) which present in the natural fiber using chemical analysis. These are the primary components of natural fibers. All chemical analysis tests were performed in accordance with ASTM-D3822 and IS199 international standards⁸². Both natural and synthetic fibers are currently used in the production of engineering materials. As a result, their mechanical and thermal characteristics depend on the environment. Therefore, in-depth research must be done to analyse the characteristics of natural fibers.

Specimen collection

The Acacia pennata plant has spread and grown throughout Kerala and Tamil Nadu in India. Acacia pennata plant for the research purposes are collected from the authors farm at Panchamoodu and Vellarada.

Guidelines and regulations

All testing was performed in accordance with the relevant ISO standards. The methods and procedures used were compliant with the guidelines and regulations outlined in the ISO standard to ensure accurate and reliable results.

Results and discussion

Powder XRD analysis

Figure 2 depicts the X-ray diffraction (XRD) pattern of the untreated and KMnO_4 -treated AP fibers. It (untreated APF) shows the crystalline peak (22.59°) on the crystallographic plane (002) and amorphous peak (15.25°) on the lattice plane (110), which demonstrates the semi-crystalline nature⁷⁷. This is because hemicellulose, lignin, and pectin are present. Two well-defined diffraction peaks are observed in KMnO_4 treated APFs around $2\theta = 22.73^\circ$ and the amorphous peak at $2\theta = 15.37^\circ$ include lignin, pectin, hemicellulose, and amorphous cellulose, which contains a larger percentage of amorphous fraction⁸³. The crystallinity index of KMnO_4 treated fiber was determined as 64.47%. The high crystallinity index of AP fiber was caused by the efficient removal of contaminants and hemicellulose. It was slightly increased when compared to untreated (46.52%) AP fiber. The CI of permanganate treated AP fibers are significantly greater than Kapok (45%) fiber and substantially lower than crushed guadua (65.3) fiber, jute (71%) and hemp (88%) fiber^{31,84}. However, using the well-known scherrer formula, the crystallite size (CS) of the KMnO_4 treated APFs was found to be 6.75 nm and it was higher than that of untreated (1.9 nm) AP fiber. The crystalline size value is lower than that of ramie fibres (16 nm) and higher than that of cotton fibers (5.5 nm), tamarindus indica fruit fibers (5.73 nm), ferula communis (1.6 nm), and carbon fibers (0.669 nm)^{85,86}. Table 1 represents the comparison of CI and CS values of raw and KMnO_4 treated APFs with other natural fibers.

FTIR analysis

Figure 3 displays the FTIR spectra of the AP fiber that had been treated with KMnO_4 . From graph, the hydrogen-bonded OH stretching group of the water molecules is responsible for the prominent peak at 3435 cm^{-1} . The CH stretching vibrations in the cellulose and hemicellulose components are visible in the peak at 2924.41 cm^{-1} . The sharp and medium peak, which is associated with the C=H stretching, lies at a height of 1645.35 cm^{-1} ⁹³. A hydrogen bond may be seen at the peak at 1420.62 cm^{-1} . The C=O stretching of lignin is what causes the absorption band at 1030.61 cm^{-1} to exist. The presence of saline content may be seen in the lower peak at 778.48 cm^{-1} . The peak at 629.07 cm^{-1} demonstrates the region of -OH bending was found at out of plane, proving that the chemical

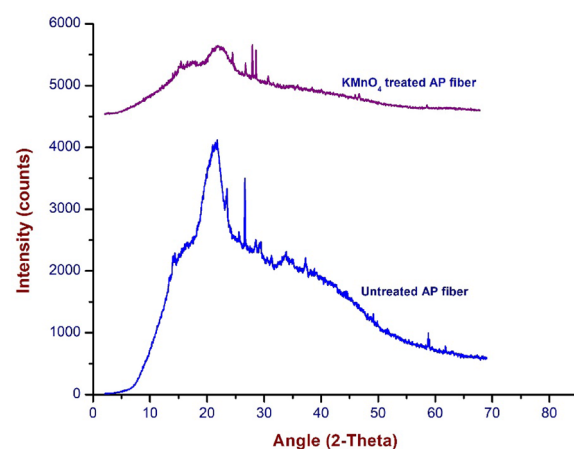


Figure 2. PXRD patterns of untreated and KMnO_4 treated AP fiber.

Fiber name	CI (%)	CS (nm)	References
Untreated AP	46.52	1.9	Present study
KMnO_4 treated AP	64.47	6.75	Present study
Ceiba pentandra	57.94	22.48	⁸⁷
Celosia argentea	52.54	3.46	⁸⁸
Bauhinia purpurea	65.61	2.57	⁸⁹
Acacia nilotica	44.82	3.21	⁹⁰
Prosopis juliflora	46	15	⁶⁹
Sida cordifolia	56.92	18	⁹¹
Leucaena leucocephala	63.10	2.33	⁹²

Table 1. Comparison table for CI and CS values of raw and KMnO_4 treated APFs with other natural fibers.

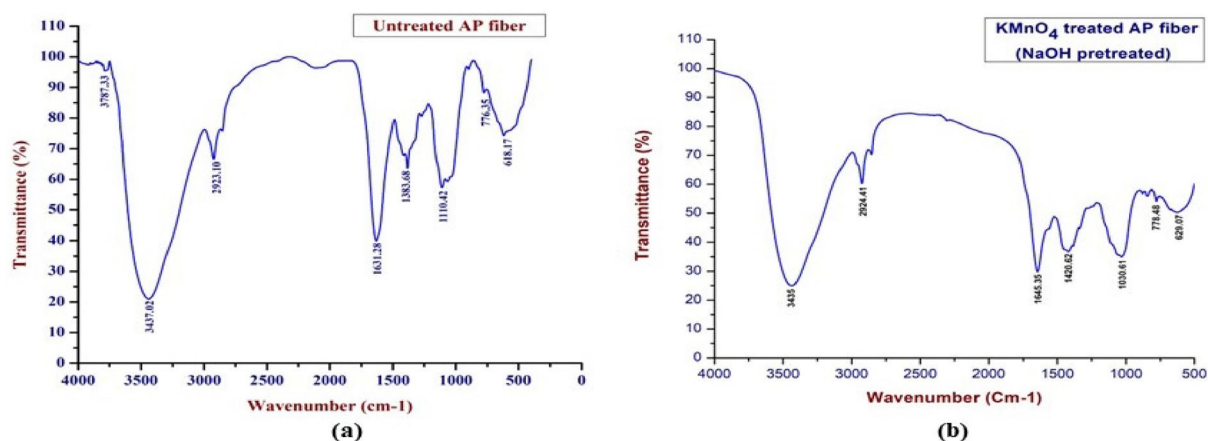


Figure 3. FTIR Spectra of untreated and KMnO_4 treated AP fiber.

analysis's findings are supported by the elimination of lignin and hemicelluloses from the KMnO_4 treated APFs. The FTIR vibrational band assignments of untreated and KMnO_4 treated AP fibers were shown in Table 2.

SEM analysis

A test method called scanning electron microscopy uses an electron beam to magnify and examine a material. The surface shape of the untreated and KMnO_4 treated AP fiber is shown in Fig. 4a,b. It was observed that the APF treated with KMnO_4 had a rough and disorganised surface shape compared with untreated APFs. It reveals that the hemicellulose content (white layer on the surface of untreated SEM image), void spaces, holes, parenchyma cells and few impurities are visible on its surface. To enhance the interfacial adhesion with polymer matrices, these hemicelluloses and lignin, wax like impurities, amorphous content should be removed, and it was done by KMnO_4 treatment. Structural properties and its modifications done by this treatment reveals that the experimental fibers can act as a good reinforcement material in composite manufacturing.

Thermo-gravimetric analysis

The weight loss of composites in relation to temperature increase was quantified using the thermo-gravimetric analysis. Greater thermal stability results from higher decomposition temperatures¹⁰⁴. The TG and DTG curves of the KMnO_4 treated APF sample was shown in Figs. 5 and 6. According to the graph, the degradation peaks are related to moisture evaporation, the breakdown of cellulose, lignin, wax, and other contaminants, as well as hemicellulose. At a temperature of about 40 °C to 120 °C, nearly 12% of weight loss has been occurred, which was mainly depending upon the moisture content in the untreated APF sample. Then the second major degradation occurs between 120 °C and 280 °C temperature range with the reduction of 18.5%. This weight loss has been observed due to the degradation of hemicellulose component. Within the temperature range between 280 °C and 400 °C, 25.46% of weight has been reduced. The destruction of the cellulose content's glycosidic linkages was the cause of the significant weight loss. Another drop was observed at the temperature within the range from 400 °C to 500 °C, nearly 20.93% of loss has occurred, which may be due to the degradation of lignin contents. Finally, degradation between 500 °C and 600 °C, due to the weight reduction of 9.5% due to the loss of wax like substances behind leaving the residue.

Wave number (cm^{-1})		Vibrational band assignments
KMnO_4 treated APF	Untreated APF	
–	3787.33	–OH Stretching in Hydrogen bond ⁹³
3435	3437.02	–Hydrogen bonded of OH stretching in cellulose and/or hemicelluloses ^{3, 94–97}
2924.41	2923.10	–CH Stretching of Cellulose ^{97–99}
1645.35	–	–C=O Stretching of a keton ¹⁰⁰
–	1631.28	–CC stretching of lignin ⁹³
1420.62	–	–Existence of CH bond ^{94, 96, 101}
–	1383.68	–Stretching in CH bond ^{97, 101}
–	1110.42	–COC pyranose ring skeletal vibration of cellulose ¹⁰²
1030.61	–	–C=O stretching of lignin ^{95, 103}
778.48	776.35	Presence of saline content ^{58, 82}
629.07	618.17	Out of plane of –OH bonding ^{58, 82}

Table 2. FTIR Vibrational band assignments of untreated KMnO_4 treated AP fibers.

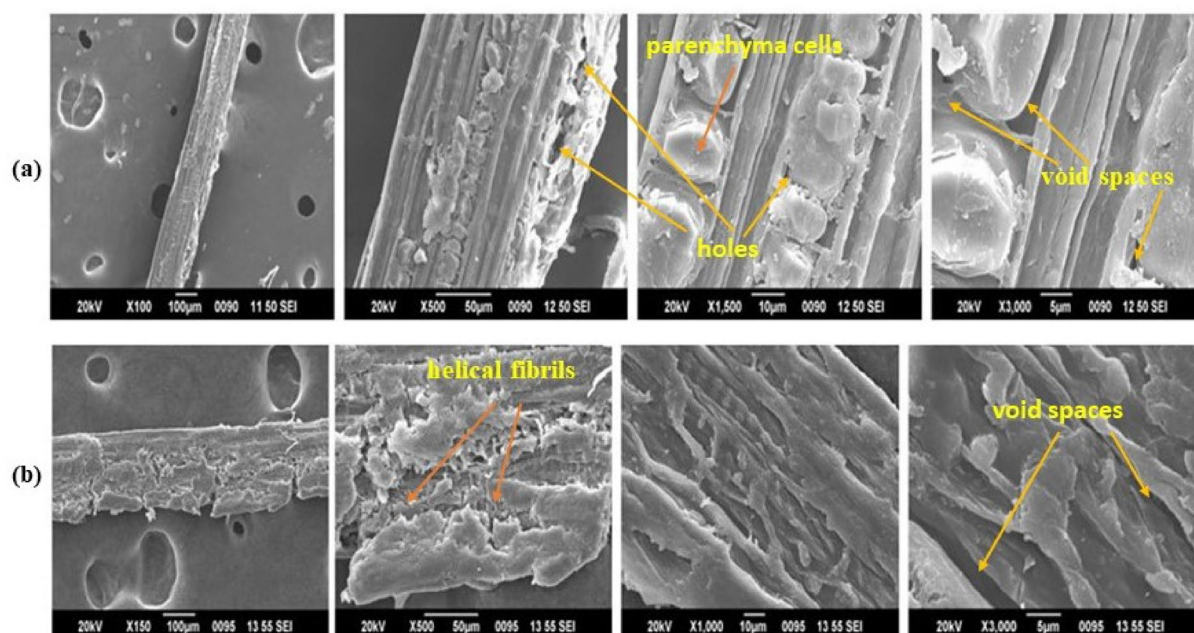


Figure 4. (a,b) Surface morphology of untreated and KMnO_4 treated AP fiber under 100, 500, 1500 and 3000 magnification fields.

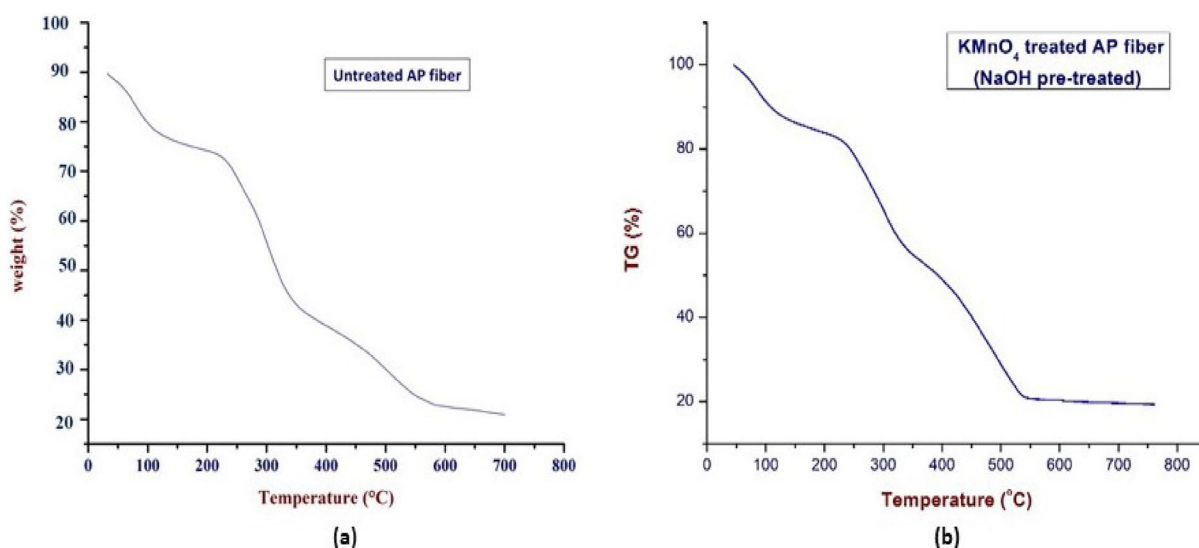


Figure 5. TG curves of untreated and KMnO_4 treated AP fiber.

In the DTG (Derivative thermo-gravimetric) curve, where the weight loss abruptly occurs at 90.7°C with a weight loss of 0.283 mg/min , clearly shows the removal of moisture content within the fiber and the second and third degradation peaks were observed at the temperatures of 259.4°C , 302.6°C , 441.2°C with the weight losses of 0.478 mg/min and 0.529 mg/min , 0.462 mg/min . Compared to hemicellulose and cellulose degradation, the thermal decomposition of lignin occurs over a wider temperature range, starts earlier, and goes up to higher temperatures 400°C ¹⁰⁵. An abrupt drop in the DTG curve, which is related to the thermal breakdown of hemicelluloses and glycosidic linkages in cellulose, serves as an indicator of this¹⁰⁶. Hemicellulose is a type of polysaccharide that is linked to cellulose and contains various sugar units. Compared to cellulose, it has a higher degree of chain branching but significantly lower levels of polymerization. Hemicellulose thermal degradation occurs before that of cellulose, although its impact is proportionally reduced by the amount of hemicellulose in the fiber¹⁰⁷.

The next deterioration peak occurred at 603.9°C with weight losses of 0.040 mg/min , which may have been caused by the breakdown of the fiber's lignin and wax components. Lignin is a complex hydrocarbon polymer that contains both aliphatic and aromatic components¹⁰⁸. Compared to the thermal decomposition of hemicellulose and cellulose, the thermal decomposition of lignin occurs over a wider range, starts earlier, and goes to higher

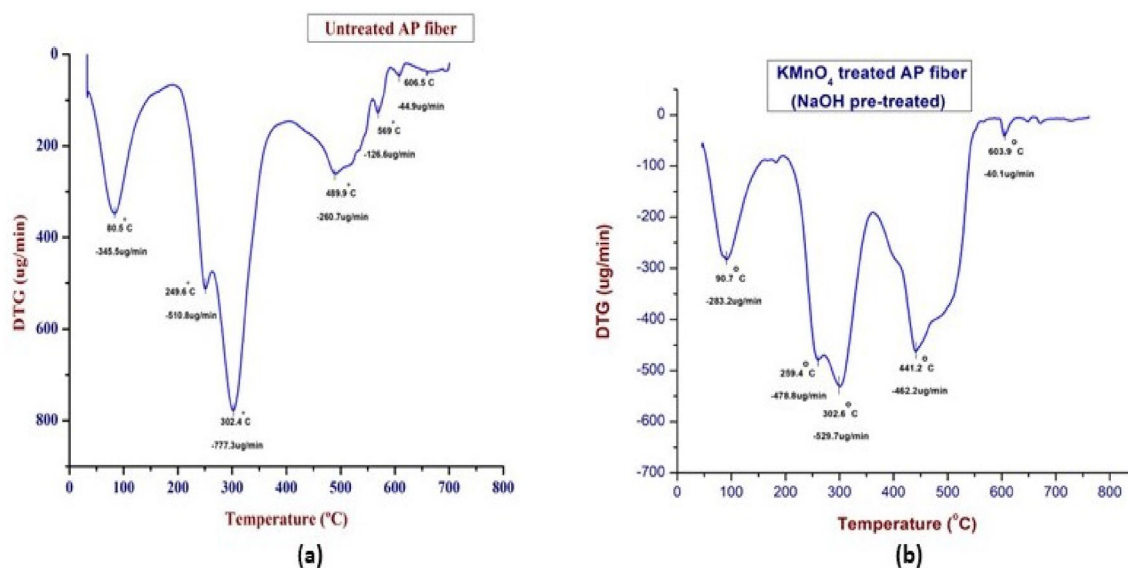


Figure 6. DTG curves of untreated and KMnO_4 treated AP fibers.

temperatures. The lesser amount of fiber present, however, also limits its impact¹⁰⁷. When the temperature ranges from ambient temperature to more than 600 °C, the complex aromatic ring component of the lignin structure decomposes with a minimum weight loss rate^{9, 109}. Tables 3 and 4 depicts the comparison between the thermal study (3) and Mass loss at Tmax (4) of untreated and KMnO_4 treated AP fibers.

Physical analysis

The density of the fiber treated with untreated and KMnO_4 was estimated to be 1090 kg/m^3 and 520 kg/m^3 (Table 6). Cavities and holes were removed during alkalization¹¹⁰. So that, density of the optimally treated APF were slightly decreased. However, the density is slightly lower than that of the *Acacia leucophloea* 1385 kg/m^3 , coir fiber 1200 kg/m^3 ³²². Due of the uneven profiles of bark fibers, diameter determination in the stem of AP fiber is rather difficult. The measured diameter of the ACF was 299.39 μm which was confirmed from SEM images. The Comparison of diameter and density values of untreated and KMnO_4 treated APFs with other natural fibers are represented in Table 5.

Type of fiber	Temperature during loss (°C)	Weight loss (%)	Thermal stability (°C)	Residual char at 750 °C
Untreated AP fibers	40–120	14.27	328.95	0.072
	120–280	20.41		
	280–400	30.32		
	400–500	11.77		
	500–600	9.91		
KMnO_4 treated AP fibers	40–120	12	337.47	0.02
	120–280	18.5		
	280–400	25.46		
	400–500	20.93		
	500–600	9.5		

Table 3. Thermal study of untreated and KMnO_4 treated AP fibers.

Type of fiber	Total mass lost (%)					Tmax (°C)
	1st stage	2nd stage	3rd stage	4th stage	5th stage	
Untreated AP fibers	14.27	34.68	65	76.77	86.88	226.3
KMnO_4 treated AP fibers	12	30.5	55.96	76.89	86.39	223.5

Table 4. Mass loss at Tmax of untreated and KMnO_4 treated AP fibers.

Fiber name	Density (g/cm ³)	Diameter (μm)	References
Untreated APF	1.09	299.39	Present study
KMnO ₄ treated APF	1.05	306.72	Present study
Date	0.99	155–250	⁵⁷
Bamboo	0.91	240–330	¹¹¹
Agave	1.20	126–344	¹¹²
Sea grass	1.50	5	¹¹³
Palm	1.03	400–490	⁵⁷
Kenaf bast	1.31	65–71	¹¹⁴
Curaua	1.40	170	^{111, 115}

Table 5. Comparison table for diameter and density values of raw and KMnO₄ treated APFs with other natural fibers.

Fiber name	N%	C%	S%	H%
Untreated AP fiber	0.76	43.38	0.51	6.75
KMnO ₄ treated AP fiber	0.80	33.22	ND	4.61

Table 6. Weight percentage of C, H, N, S in untreated and KMnO₄ treated AP fiber. *ND* not detected.

CHNS analysis

The Dumas's method⁵⁸, which entails the total and rapid oxidation of the sample by "flash combustion," is the basis for the CHNS analyser, which is used to determine the percentages of carbon, hydrogen, nitrogen, and sulphur in organic compounds. The Dumas method is a technique for calculating the quantity of chemical compounds (elements). This approach is most useful for figuring out how much C, H, N, and S are present in organic compounds, which typically ignite at 1800 °C. The weight percentage of each chemical in the KMnO₄ treated sample is displayed in Table 6.

According to CHNS study, untreated AP fibres have a carbon content of 43.38%, however after being treated with permanganate, the carbon content decreases to 33.22%. One of the most vital aspects to alter the mechanical and tribological qualities of the final product is high carbon content in the natural fibers. Both samples can be employed as conductive fillers in dielectric loss materials because of the carbon content is above 30% in both. The average composition of carbon and hydrogen in chicken feather fibres are 47.4% and 7.2%¹¹⁶. It is found that the carbon content of coconut shell fibres and sugarcane bagasse fibres are 46.7% and 44.7%. These values are comparable to AP fibers.

Chemical analysis

Table 7 provides the comparison table of chemical composition of untreated, KMnO₄ treated with different existing fibers. After pre-treatment, the cellulose content of the plant fibers generally increased. Due to the crystalline areas' altered lattice structures, the APF has a cellulose content of 55.4%¹¹⁷. These fibers have lower cellulose levels than Acacia Concinna fiber (59.43 wt%), Acacia leucophloea (68.09 wt% to 76.69 wt%), and Prosopis Juliflora fiber (61.65 wt% to 72.27 wt%)⁹³ and larger than that of coir fiber (32–43%) and Ficus leaf fiber (38.1%)^{93, 118}. Hemi-Cellulose of the APF was decreased (13.30%) in this treatment. This hemicellulose content was much larger than that of Acacia concinna fiber (12.78%) and Acacia planifrons (9.41%) etc. The diffusion of lignin in KMnO₄ solution was blamed for the significant change in the lignin concentration (17.75%). However, it is soluble in hot alkali, rapidly oxidised, and condensable with phenol. Lignin is not hydrolyzed by acids¹¹⁹. After this treatment, pectin levels similarly dropped (1.9%). Wax content (0.79%) of the KMnO₄-treated APF dropped as well, which is a favourable change. As opposed to plant fiber with higher wax content, fiber from plants with

Fiber name	Cellulose (%)	Hemi-cellulose (%)	Lignin (%)	Pectin (%)	Wax (%)	Moisture (%)	Ash (%)	References
Untreated APF	45.68	41.13	24.49	12.19	13.91	0.36	3.13	Present work
KMnO ₄ treated APF	55.4	13.3	17.75	1.9	13.4	0.79	10	Present work
Kenaf fiber	45–57	8–13	21.5	0.6	0.8	6.2–12	2–5	^{121, 122}
Wheat husk	36	18	16	–	–	–	–	¹²³
Sisal fiber	78	10	8	–	2	11	1	¹²⁴
Agave fiber	68.42	4.85	4.85	–	0.26	7.69	–	¹²⁵
Corn straw fiber	44.5	19.7	25.5	1.4	–	–	–	¹²¹

Table 7. Comparison table of chemical compositions of APFs with other existing fibers.

reduced wax content can produce excellent interfacial bonds with polymers¹²⁰. The amount of moisture (13.4%) in the KMnO₄-treated APF decreased as well. The ash content of the APF, on the other hand, was subtly increased from 10%, which supported the growth of the crystalline component in the fiber¹¹⁰.

Tensile strength

One of the most often investigated features of natural fiber reinforced composites is tensile strength. When choosing a particular natural fiber for a given application, the fiber strength can be a crucial consideration¹²⁶. Tensile testing of individual technical fibers is a standard method for determining the tensile characteristics of natural fibers¹²⁷. The test was conducted at an ambient temperature of 21 °C, a relative humidity of approximately 65%, and a specimen gauge length of 50 mm¹⁰⁰. The comparison of tensile strength, young's modulus, micro-fibrillar angle, and breaking elongation of the untreated and KMnO₄-treated APFs with other natural fibers are shown in Table 8. According to the computed data, the tensile strength of the untreated and KMnO₄ treated APFs were found to 181.69 MPa and 685 MPa with 6.2%, 4.1% elongation and young's modulus 29.3GPa, 16.707 GPa respectively. The tensile strength of the jute fiber is (400–800 MPa) and its young's modulus is (10–30 GPa)¹²⁸. As a result, the AP fiber's tensile strength and young's modulus were almost on par with those of jute fiber. The cell walls structure and chemical makeup of bark fibers, particularly the amount of cellulose, have a significant impact on their mechanical properties¹²⁹.

Conclusion

The paper discusses the outcomes of analyses performed on the KMnO₄-treated AP fiber using X-ray diffraction (XRD), Fourier Transform Infrared (FTIR), scanning electron microscopy (SEM), thermo-gravimetric analysis (TGA), and mechanical (tensile strength) analysis.

- (1) The mechanical analysis of AP fiber makes it a dependable and long-lasting material for building composite fiber materials and fiber reinforced concrete for use in construction. Due to the orientation of the fibers, AP fibers have superior mechanical properties (such strength and young's modulus), which improves their capacity to handle loads and stress.
- (2) The KMnO₄-treated AP fiber's X-ray diffraction (XRD) patterns revealed a semi-crystalline structure, with a crystallinity index of 51.63%. These findings imply that the KMnO₄ treatment was successful in eliminating impurities and raising the AP fiber's crystallinity index. The crystallite size of the KMnO₄-treated AP fiber was 1.05 nm. Overall, the results of this study provide valuable information on the effects of KMnO₄ treatment on the structure, stability and mechanical analysis of AP fiber.
- (3) FTIR spectral analysis revealed the existence of lignin, saline content, and components of cellulose and hemicellulose. Scanning electron microscopy revealed that the KMnO₄-treated AP fiber's surface was rough and disordered, with amorphous content and impurities clearly apparent. Chemical analysis outcomes showed that APF has the higher cellulose (55.4%) and lesser hemicellulose (13.3%) content.
- (4) The degradation of moisture, cellulose, lignin, wax, and other impurities, as well as hemicellulose, corresponded to the peaks in the thermo-gravimetric study. This thermo-gravimetric analysis showed that the KMnO₄ treated AP fiber has a higher thermal stability (337.47 °C), with higher decomposition temperatures (223.5 °C), making it a potential candidate for use in composite materials.
- (5) This fiber's overall structure and stability have improved as a result of the KMnO₄ treatment. Therefore, with further purification, AP fibre has the potential to be used as a reinforcement material in the creation of composites. All the above findings and lower density (520 kg/m³) of the APF would make them suitable for lightweight composite materials.

The experiments conducted on KMnO₄ treated *Acacia pennata* fibers show remarkable mechanical properties, such as tensile strength of 685 MPa and a Young's modulus of 16.707 GPa. The high tensile strength of *Acacia pennata* fibers has a possibility of utilizing as particle replacement of cementitious material in the construction as well as interior structural components. In the current practices many natural fibers are utilized in the construction sector. Furthermore, these composites have high potential to be applied in the sandwich structure due to

Fiber name	Tensile strength (MPa)	Young's modulus (GPa)	Micro-fibrillar angle (°)	Elongation at break (%)	References
Untreated APF	181.69 ± 40	29.30 ± 3	19.67 ± 3	6.2	Present study
KMnO ₄ treated APF	685 ± 60	16.707 ± 7	16.134 ± 5	4.1	Present study
Zea mays	13.243	0.529	12.68	2.5	59
Ficus racemosa	270	67.45	–	2.57	130
Hemp	690	70	6.2	1.6	131
Butea parviflora	198.12	4.4	16.88 ± 9.87	4.5	132
Heteropogon contortus	476 ± 11.6	48 ± 2.8	14.53 ± 0.53	–	133
Cissus quadrangularis	200.39	4.89	–	3.57–8.37	51
Banana	700–800	27–32	–	–	133

Table 8. Comparison table for Tensile strength of untreated and KMnO₄ treated APFs with other natural fibers.

its light weight with higher flexural properties. The fibers microfibrillar angle of 16.134° and break elongation of 4.1% further support their suitability for these applications. However, it is crucial to evaluate these results against industry standards to fully assess the potential of the *Acacia pennata* fibers applications. Further research should be conducted to examine their feasibility and performance against existing materials in the construction and composite industries.

Data availability

The datasets generated during and/or analysed during the current study are available from the author and corresponding author on reasonable request.

Received: 23 March 2023; Accepted: 6 November 2023

Published online: 24 November 2023

References

- Mwaikambo, L. Y. & Ansell, M. P. Chemical modification of hemp, sisal, jute, and kapok fibers by alkalization. *J. Appl. Polym. Sci.* **84**, 2222–2234 (2002).
- Bernard, M. *et al.* The effect of processing parameters on the mechanical properties of kenaf fibre plastic composite. *Mater. Des.* **32**, 1039–1043 (2011).
- Céline, A., Gonçalves, O., Jacquemin, F. & Fréour, S. Qualitative and quantitative assessment of water sorption in natural fibres using ATR-FTIR spectroscopy. *Carbohydr. Polym.* **101**, 163–170 (2014).
- Pal, D. B. *et al.* Enhanced biogas production potential analysis of rice straw: Biomass characterization, kinetics and anaerobic co-digestion investigations. *Bioresour. Technol.* **358**, 127391 (2022).
- Tiwari, Y. M. & Sarangi, S. K. Comprehensive characterization of new natural fiber extracted from the stem of *Grewia flavescens* plant. *J. Nat. Fibers* **19**, 14579–14591 (2022).
- Gopinath, R., Billigraham, P., Sathishkumar, T. P. & Rajasekar, R. Physicochemical, thermal and mechanical properties of novel cellulosic fiber extracted from *Ficus retusa*. *J. Nat. Fibers* **19**, 14706–14724 (2022).
- Machaka, M., Abou Chakra, H. & Elkordi, A. Alkali treatment of fan palm natural fibers for use in fiber reinforced concrete. *Eur. Sci. J.* **10**, 186–195 (2014).
- Gopinath, R., Billigraham, P. & Sathishkumar, T. P. Characterization studies on novel cellulosic fiber obtained from the bark of *Madhuca longifolia* tree. *J. Nat. Fibers* **19**, 14880–14897 (2022).
- Derosa, M., Monreal, C., Schnitzer, M., Walsh, R. & Sultan, Y. Nanotechnology in fertilizers. *Nat. Nanotechnol.* **5**, 91 (2010).
- Ramesh, M. *et al.* Influence of Haritaki (*Terminalia chebula*) nano-powder on thermo-mechanical, water absorption and morphological properties of Tindora (*Coccinia grandis*) tendrils fiber reinforced epoxy composites. *J. Nat. Fibers* **19**, 6452–6468 (2022).
- Ramesh, M. *et al.* Impact of silane treatment on characterization of *Ipomoea staphylina* plant fiber reinforced epoxy composites. *J. Nat. Fibers* **19**, 5888–5899 (2022).
- Sivasubramanian, P. *et al.* Effect of alkali treatment on the properties of *Acacia caesia* bark fibres. *Fibers* **9**, 49 (2021).
- Kim, H. S., Park, Y. H., Kim, S. & Choi, Y.-E. Application of a polyethylenimine-modified polyacrylonitrile-biomass waste composite fiber sorbent for the removal of a harmful cyanobacterial species from an aqueous solution. *Environ. Res.* **190**, 109997 (2020).
- Nagappan, S., Subramani, S. P., Palaniappan, S. K. & Mylsamy, B. Impact of alkali treatment and fiber length on mechanical properties of new agro waste Lagenaria Siceraria fiber reinforced epoxy composites. *J. Nat. Fibers* **19**, 6853–6864 (2022).
- Shaker, K. *et al.* Cellulosic fillers extracted from *Argyrea speciosa* waste: A potential reinforcement for composites to enhance properties. *J. Nat. Fibers* <https://doi.org/10.1080/15440478.2020.1856271> (2020).
- Shaker, K. *et al.* Extraction and characterization of novel fibers from *Vernonia elaeagnifolia* as a potential textile fiber. *Ind. Crops Prod.* **152**, 112518 (2020).
- Mylsamy, B., Chinnsamy, V., Palaniappan, S. K., Subramani, S. P. & Gopalsamy, C. Effect of surface treatment on the tribological properties of *Coccinia Indica* cellulosic fiber reinforced polymer composites. *J. Mater. Res. Technol.* **9**, 16423–16434 (2020).
- Aruchamy, K. *et al.* Effect of blend ratio on the thermal comfort characteristics of cotton/bamboo blended fabrics. *J. Nat. Fibers* **19**, 105–114 (2022).
- Bhuvaneshwaran, M., Sampath, P. S. & Sagadevan, S. Influence of fiber length, fiber content and alkali treatment on mechanical properties of natural fiber-reinforced epoxy composites. *Polimery/Polymers* **64**, 93–99 (2019).
- Bhuvaneshwaran, M., Subramani, S. P., Palaniappan, S. K., Pal, S. K. & Balu, S. Natural cellulosic fiber from *Coccinia indica* stem for polymer composites: Extraction and characterization. *J. Nat. Fibers* **18**, 644–652 (2021).
- Shaker, K., Nawab, Y. & Jabbar, M. Bio-composites: Eco-friendly substitute of glass fiber composites. *Handb. Nanomater. Nano-composites Energy Environ. Appl.* (2021).
- Nurwidayati, R. & Azima, N. N. Utilization of coconut shell ash as a substitute material in paving block manufacturing. *IOP Conf. Ser. Earth Environ. Sci.* **999**, 012009 (2022).
- Holbery, J. & Houston, D. Natural-fiber-reinforced polymer composites in automotive applications. *JOM* **58**, 80–86 (2006).
- Bledzki, A. K., Faruk, O. & Sperber, V. E. Cars from bio-fibres. *Macromol. Mater. Eng.* **291**, 449–457 (2006).
- Awoyera, P. O. *et al.* Experimental findings and validation on torsional behaviour of fibre-reinforced concrete beams: A review. *Polymers* **14**, 1171 (2022).
- Avudaiappan, S. *et al.* Innovative use of single-use face mask fibers for the production of a sustainable cement mortar. *J. Compos. Sci.* **7**, 214 (2023).
- Céline, A., Fréour, S., Jacquemin, F. & Casari, P. The hygroscopic behavior of plant fibers: A review. *Front. Chem.* **1**, 1–12 (2014).
- Sonawane, G. H., Patil, S. P. & Sonawane, S. H. Nanocomposites and its applications. In *Micro and Nano Technologies* (eds Mohan Bhagyaraj, S. *et al.*) 1–22 (Woodhead Publishing, 2018).
- Meneghetti, P. & Qutubuddin, S. Synthesis, thermal properties and applications of polymer-clay nanocomposites. *Thermochim. Acta* **442**, 74–77 (2006).
- Sheeba, K. R. J. *et al.* Characterisation of sodium acetate treatment on *Acacia pennata* natural fibres. *Polymers* **15**, 1996 (2023).
- Paul, O. A. *et al.* Structural retrofitting of corroded reinforced concrete beams using bamboo fiber laminate. *Materials* **14**, 6711 (2021).
- Arunachalam, K. P., Avudaiappan, S., Flores, E. I. S. & Parra, P. F. Experimental study on the mechanical properties and microstructures of cenosphere concrete. *Materials* **16**, 3518 (2023).
- Komuraiah, A., Kumar, N. S. & Prasad, B. D. Chemical composition of natural fibers and its influence on their mechanical properties. *Mech. Compos. Mater.* **50**, 359–376 (2014).
- Ahmad, R., Hamid, R. & Osman, S. A. Physical and chemical modifications of plant fibres for reinforcement in cementitious composites. *Adv. Civ. Eng.* **2019**, 5185806 (2019).

35. Peças, P., Carvalho, H., Salman, H. & Leite, M. Natural fibre composites and their applications: A review. *J. Compos. Sci.* **2**, 1–20 (2018).
36. Kaushik, V., Kumar, A. & Kalia, S. Effect of mercerization and benzoyl peroxide treatment on morphology, thermal stability and crystallinity of sisal fibers. *Int. J. Text. Sci.* **1**, 101–105 (2013).
37. Abisha, M. *et al.* Biodegradable green composites: Effects of potassium permanganate (KMnO₄) treatment on thermal, mechanical, and morphological behavior of *Butea parviflora* (BP) fibers. *Polymers* **15**, 2197 (2023).
38. Liew, M. S., Nguyen-Tri, P., Nguyen, T. A. & Kakooei, S. *Smart Nanoconcretes and Cement-Based Materials* (2020).
39. Segal, L., Creely, J. J., Martin, A. E. & Conrad, C. M. An empirical method for estimating the degree of crystallinity of native cellulose using the X-ray diffractometer. *Text. Res. J.* **29**, 786–794 (1959).
40. Gurukarthik Babu, B., Prince Winston, D., SenthamaraiKannan, P., Saravanakumar, S. S. & Sanjay, M. R. Study on characterization and physicochemical properties of new natural fiber from *Phaseolus vulgaris*. *J. Nat. Fibers* **16**, 1035–1042 (2019).
41. Amutha, V. & Kumar, S. Physical, chemical, thermal, and surface morphological properties of the bark fiber extracted from *Acacia concinna* plant. *J. Nat. Fibers* **18**, 1–14 (2019).
42. Abdul Samad Khan, A. A. C. *Handbook of Ionic Substituted Hydroxyapatites* (2020).
43. Rivera-Gómez, C., Galán-Marín, C. & Bradley, F. Analysis of the influence of the fiber type in polymer matrix/fiber bond using natural organic polymer stabilizer. *Polymers* **6**, 977–994 (2014).
44. Arunachalam, K. P. *et al.* Innovative use of copper mine tailing as an additive in cement mortar. *J. Mater. Res. Technol.* <https://doi.org/10.1016/j.jmrt.2023.06.066> (2023).
45. Arunachalam, K. P. & Henderson, J. H. Experimental study on mechanical strength of vibro-compacted interlocking concrete blocks using image processing and microstructural analysis. *Iran. J. Sci. Technol. Trans. Civ. Eng.* <https://doi.org/10.1007/s40996-023-01194-8> (2023).
46. RajeshKumar, K. *et al.* Structural performance of biaxial geogrid reinforced concrete slab. *Int. J. Civ. Eng.* **20**, 349–359 (2022).
47. Abraham, J., Mohammed, A. P., Ajith Kumar, M. P., George, S. C. & Thomas, S. Thermoanalytical techniques of nanomaterials. In *Micro and Nano Technologies* (eds Mohan Bhagyaraj, S. *et al.*) 213–236 (Woodhead Publishing, 2018).
48. Moshi, A. A. M. *et al.* Characterization of a new cellulosic natural fiber extracted from the root of *Ficus religiosa* tree. *Int. J. Biol. Macromol.* **142**, 212–221 (2020).
49. Ravindran, D. *et al.* Characterization of natural cellulosic fiber extracted from *Grewia damine* flowering plant's stem. *Int. J. Biol. Macromol.* **164**, 1246–1255 (2020).
50. SenthamaraiKannan, P. & Kathiresan, M. Characterization of raw and alkali treated new natural cellulosic fiber from *Coccinia grandis* L. *Carbohydr. Polym.* **186**, 332–343 (2018).
51. Siva, R. *et al.* Characterization of mechanical, chemical properties and microstructure of untreated and treated *Cissus quadrangularis* fiber. *Mater. Today Proc.* **47**, 4479–4483 (2021).
52. Subramanian, S. G., Rajkumar, R. & Ramkumar, T. Characterization of natural cellulosic fiber from *Cereus hildmannianus*. *J. Nat. Fibers* **18**, 343–354 (2021).
53. Indran, S. & Raj, R. E. Characterization of new natural cellulosic fiber from *Cissus quadrangularis* stem. *Carbohydr. Polym.* **117**, 392–399 (2015).
54. Siva, R., Valarmathi, T. N., Palanikumar, K. & Samrot, A. V. Study on a Novel natural cellulosic fiber from *Kigelia africana* fruit: Characterization and analysis. *Carbohydr. Polym.* **244**, 116494 (2020).
55. Herlina Sari, N., Wardana, I. N. G., Irawan, Y. S. & Siswanto, E. Characterization of the chemical, physical, and mechanical properties of NaOH-treated natural cellulosic fibers from corn husks. *J. Nat. Fibers* **15**, 545–558 (2018).
56. Manimaran, P., Pillai, G. P., Vignesh, V. & Prithiviraj, M. Characterization of natural cellulosic fibers from Nendran Banana Peduncle plants. *Int. J. Biol. Macromol.* **162**, 1807–1815 (2020).
57. Rao, K. M. M. & Rao, K. M. Extraction and tensile properties of natural fibers: Vakka, date and bamboo. *Compos. Struct.* **77**, 288–295 (2007).
58. Sheeba, K. R. J. *et al.* Physico-chemical and extraction properties on alkali-treated *Acacia pennata* fiber. *Environ. Res.* **233**, 116415 (2023).
59. Kavitha, S. A. *et al.* Investigation on properties of raw and alkali treated novel cellulosic root fibres of *Zea mays* for polymeric composites. *Polymers* **15**, 1802 (2023).
60. Velmurugan, G., Vadivel, D., Arravind, R., Mathiazhagan, A. & Vengatesan, S. P. Tensile test analysis of natural fiber reinforced composite. *Int. J. Mech. Ind. Eng.* **3**, 148–152 (2014).
61. Horst, C. *et al.* Springer handbook of materials measurement methods. *Mater. Today* **9**, 52 (2006).
62. Moigne, N., Otazaghine, B., Corn, S., Angellier-Coussy, H. & Bergeret, A. *Characterization of the Fibre Modifications and Localization of the Functionalization Molecules* 71–100 (Springer, 2018).
63. Ganapathy, T., Sathiskumar, R., SenthamaraiKannan, P., Saravanakumar, S. S. & Khan, A. Characterization of raw and alkali treated new natural cellulosic fibres extracted from the aerial roots of banyan tree. *Int. J. Biol. Macromol.* **138**, 573–581 (2019).
64. Oladele, I. O., Michael, O. S., Adediran, A. A., Balogun, O. P. & Ajagbe, F. O. Acetylation treatment for the batch processing of natural fibers: Effects on constituents, tensile properties and surface morphology of selected plant stem fibers. *Fibers* **8**, 73 (2020).
65. Mishra, S., Prabhakar, B., Kharkar, P. S. & Pethe, A. M. Banana peel waste: An emerging cellulosic material to extract nanocrystalline cellulose. *ACS Omega* **8**, 1140–1145 (2023).
66. Mendes, C. A., Adnet, F., Leite, M. C. A. M., Furtado, C. & Maria, F. Chemical, physical, mechanical, thermal and morphological characterization of corn husk residue. *Cellul. Chem. Technol.* **49**, 727–735 (2015).
67. Baskaran, P. G., Kathiresan, M., SenthamaraiKannan, P. & Saravanakumar, S. S. Characterization of new natural cellulosic fiber from the bark of *Dichrostachys cinerea*. *J. Nat. Fibers* **15**, 62–68 (2018).
68. Babu, B. G. *et al.* Investigation on the physicochemical and mechanical properties of novel alkali-treated *Phaseolus vulgaris* fibers. *J. Nat. Fibers* **19**, 770–781 (2022).
69. Saravanakumar, S. S., Kumaravel, A., Nagarajan, T., Sudhakar, P. & Baskaran, R. Characterization of a novel natural cellulosic fiber from *Prosopis juliflora* bark. *Carbohydr. Polym.* **92**, 1928–1933 (2013).
70. Kathirselvam, M., Kumaravel, A., Arthanarieswaran, V. P. & Saravanakumar, S. S. Characterization of cellulose fibers in *Thespesia populnea* barks: Influence of alkali treatment. *Carbohydr. Polym.* **217**, 178–189 (2019).
71. Balaji, A. N. & Nagarajan, K. J. Characterization of alkali treated and untreated new cellulosic fiber from Saharan aloe vera cactus leaves. *Carbohydr. Polym.* **174**, 200–208 (2017).
72. Mohd Roslim, M. H., Sapuan, S., Leman, Z. & Ishak, M. Comparative study on chemical composition, physical, tensile, and thermal properties of sugar palm fiber (*Arenga pinnata*) obtained from different geographical locations. *BioResources* **12**, 9366–9382 (2017).
73. Tamanna, T. A., Belal, S. A., Shibly, M. A. H. & Khan, A. N. Characterization of a new natural fiber extracted from *Corypha taliera* fruit. *Sci. Rep.* **11**, 7622 (2021).
74. Nayak, S. & Mohanty, J. Influence of chemical treatment on tensile strength, water absorption, surface morphology, and thermal analysis of areca sheath fibers. *J. Nat. Fibers* **16**, 589–599 (2019).
75. Yusriah, L., Sapuan, S. M., Zainudin, E. S. & Mariatti, M. Characterization of physical, mechanical, thermal and morphological properties of agro-waste betel nut (*Areca catechu*) husk fibre. *J. Clean. Prod.* **72**, 174–180 (2014).

76. Keskin, O. Y., Dalmis, R., Balci Kilic, G., Seki, Y. & Korktas, S. Extraction and characterization of cellulosic fiber from *Centaurea solstitialis* for composites. *Cellulose* **27**, 9963–9974 (2020).
77. Belouadah, Z., Ati, A. & Rokbi, M. Characterization of new natural cellulosic fiber from *Lygeum spartum* L. *Carbohydr. Polym.* **134**, 429–437 (2015).
78. Sarala, R. Characterization of a new natural cellulosic fiber extracted from *Derris scandens* stem. *Int. J. Biol. Macromol.* **165**, 2303–2313 (2020).
79. Binoj, J. S., Raj, R. E., Sreenivasan, V. S. & Thusnavis, G. R. Morphological, physical, mechanical, chemical and thermal characterization of sustainable Indian Areca fruit husk fibers (*Areca catechu* L.) as potential alternate for hazardous synthetic fibers. *J. Bionic Eng.* **13**, 156–165 (2016).
80. DjafariPetroudy, S. R. Physical and mechanical properties of natural fibers. In *Advanced High Strength Natural Fibre Composites in Construction* (eds Fan, M. & Fu, F.) 59–83 (Woodhead Publishing, 2017).
81. Awoyera, P. O., Olalusi, O. B., Ibia, S., Prakash, A. & K., Water absorption, strength and microscale properties of interlocking concrete blocks made with plastic fibre and ceramic aggregates. *Case Stud. Constr. Mater.* **15**, e00677 (2021).
82. Sheeba, K. R. J. *et al.* Case studies in construction materials enhancing structural, thermal, and mechanical properties of *Acacia pennata* natural fibers through benzoyl chloride treatment for construction applications. *Case Stud. Constr. Mater.* **19**, e02443 (2023).
83. Arthanarieswaran, V. P., Kumaravel, A. & Saravanakumar, S. S. Physico-chemical properties of alkali-treated acacia leucophloea fibers. *Int. J. Polym. Anal. Charact.* **20**, 704–713 (2015).
84. Sanchez-Echeverri, L. A., Medina-Perilla, J. A. & Ganjian, E. Nonconventional Ca(OH)₂ treatment of bamboo for the reinforcement of cement composites. *Materials* **13**, 1892 (2020).
85. Elenga, R. G., Dirras, G. F., Goma Maniongui, J., Djemia, P. & Biget, M. P. On the microstructure and physical properties of untreated raffia textilis fiber. *Composites Part A* **40**, 418–422 (2009).
86. Binoj, J. S., Raj, R. E. & Indran, S. Characterization of industrial discarded fruit wastes (*Tamarindus indica* L.) as potential alternate for man-made vitreous fiber in polymer composites. *Process Saf. Environ. Prot.* **116**, 527–534 (2018).
87. Kumar, R., Hynes, N. R. J., Senthamaraiannan, P., Saravanakumar, S. & Sanjay, M. R. Physicochemical and thermal properties of *Ceiba pentandra* bark fiber. *J. Nat. Fibers* **15**, 822–829 (2018).
88. Manimaran, P. *et al.* Physico-chemical properties of fiber extracted from the flower of celosia argentea plant. *J. Nat. Fibers* **18**, 464–473 (2021).
89. Gopinath, R., Billigraham, P. & Sathishkumar, T. P. Investigation of physico-chemical, mechanical, and thermal properties of new cellulosic bast fiber extracted from the bark of *Bauhinia purpurea*. *J. Nat. Fibers* **19**, 9624–9641 (2022).
90. Kumar, R. *et al.* Characterization of new cellulosic fiber from the bark of *Acacia nilotica* L. *Plant. J. Nat. Fibers* **19**, 199–208 (2022).
91. Manimaran, P., Prithiviraj, M., Saravanakumar, S. S., Arthanarieswaran, V. P. & Senthamaraiannan, P. Physicochemical, tensile, and thermal characterization of new natural cellulosic fibers from the stems of *Sida cordifolia*. *J. Nat. Fibers* **15**, 860–869 (2018).
92. Gopinath, R., Billigraham, P. & Sathishkumar, T. P. Characterization studies on new cellulosic fiber extracted from leucaena leucocephala tree. *J. Nat. Fibers* **20**, 57922 (2023).
93. Khuntia, T. & Biswas, S. Characterization of a novel natural filler from Sirisha Bark. *J. Nat. Fibers* **19**, 3083–3092 (2022).
94. Fan, M., Dai, D. & Huang, B. Fourier transform infrared spectroscopy for natural fibres. *Fourier Transform Mater. Anal.* <https://doi.org/10.5772/35482> (2012).
95. Glória, G. O., de Moraes, Y. M., Margem, F. M., Vieira, C. M. F. & Monteiro, S. N. Evaluation of giant bamboo fibers components by infrared spectroscopy. *Cong Annu. ABM* <https://doi.org/10.5151/1516-392x-26322> (2017).
96. Comnea-Stancu, I. R., Wieland, K., Ramer, G., Schwaighofer, A. & Lendl, B. On the identification of rayon/viscose as a major fraction of microplastics in the marine environment: Discrimination between natural and manmade cellulosic fibers using fourier transform infrared spectroscopy. *Appl. Spectrosc.* **71**, 939–950 (2017).
97. Shi, Z., Zhu, G., Xu, H. & Chen, Y. Preparation and characterization of AC/PEDOT composites. *Gongneng Cailiao/J. Funct. Mater.* **49**, 06201–06205 (2018).
98. Sosiati, H. & Harsojo, H. Effect of combined treatment methods on the crystallinity and surface morphology of kenaf bast fibers. *Cellul. Chem. Technol.* **48**, 33–43 (2014).
99. Adeniyi, A. G., Onifade, D. V., Ighalo, J. O., Abdulkareem, S. A. & Aмосa, M. K. Extraction and characterization of natural fibres from plantain (*Musa paradisiaca*) stalk wastes. *Iran. J. Energy Environ.* **11**, 116–121 (2020).
100. Jebadurai, S. G., Raj, R. E., Sreenivasan, V. S. & Binoj, J. S. Comprehensive characterization of natural cellulosic fiber from *Cocinia grandis* stem. *Carbohydr. Polym.* **207**, 675–683 (2019).
101. Värban, R. *et al.* Comparative FT-IR prospecting for cellulose in stems of some fiber plants: Flax, velvet leaf, hemp and jute. *Appl. Sci.* **11**(18), 8570 (2021).
102. Reddy, K. O. *et al.* Extraction and characterization of novel lignocellulosic fibers from *Thespesia lampas* plant. *Int. J. Polym. Anal. Charact.* **19**, 48–61 (2014).
103. Moosavinejad, S. M., Madhoushi, M., Vakili, M. & Rasouli, D. Evaluation of degradation in chemical compounds of wood in historical buildings using Ft-Ir And Ft-Raman vibrational spectroscopy. *Maderas Cienc. Tecnol.* **21**, 381–392 (2019).
104. Neto, J. S. S. *et al.* Effect of chemical treatment on the thermal properties of hybrid natural fiber-reinforced composites. *J. Appl. Polym. Sci.* **136**, 1–13 (2019).
105. Correa, S. M., Arbilla, G., Marques, M. R. C. & Oliveira, K. M. P. G. The impact of BTEX emissions from gas stations into the atmosphere. *Atmos. Pollut. Res.* **3**, 163–169 (2012).
106. Liu, W., Mohanty, A. K., Drzal, L. T., Askel, P. & Misra, M. Effects of alkali treatment on the structure, morphology and thermal properties of native grass fibers as reinforcements for polymer matrix composites. *J. Mater. Sci.* **39**, 1051–1054 (2004).
107. Monteiro, S. & Calado, V. Thermogravimetric behavior of natural fibers reinforced polymer composites: An overview. *Mater. Sci. Eng. A* **557**, 17–28. <https://doi.org/10.1016/j.msea.2012.05.109> (2012).
108. Bledzki, A. K. & Gassan, J. Composites reinforced with cellulose based fibres. *Prog. Polym. Sci.* **24**, 221–274 (1999).
109. Selvaraj, M. *et al.* Extraction and characterization of a new natural cellulosic fiber from bark of *Ficus carica* plant as potential reinforcement for polymer composites. *J. Nat. Fibers* **20**, 2194699 (2023).
110. Devaki, E. & Boominathan, S. Physical, thermal and tensile analysis of sansiveria roxburghiana leaf fiber. *J. Nat. Fibers* **19**, 7797–7805 (2022).
111. John, M. & Anandjiwala, R. Recent developments in chemical modification and characterization of natural fiber-reinforced composites. *Polym. Compos.* **29**, 187–207 (2008).
112. Thamae, T. & Baillie, C. Influence of fibre extraction method, alkali and silane treatment on the interface of Agave americana waste HDPE composites as possible roof ceilings in Lesotho. *Compos. Interfaces* **14**, 821–836 (2007).
113. Davies, P., Morvan, C., Sire, O. & Baley, C. Structure and properties of fibres from sea-grass (*Zostera marina*). *J. Mater. Sci.* **42**, 4850–4857 (2007).
114. Sathishkumar, T. P., Navaneethakrishnan, P., Shankar, S. & Rajasekar, R. Characterization of new cellulose sansiveria ehrenbergii fibers for polymer composites. *Compos. Interfaces* **20**, 575–593 (2013).
115. Monteiro, S., Aquino, R. & Perissé Duarte Lopes, F. Performance of curaua fibers in pullout tests. *J. Mater. Sci.* **43**, 489–493 (2008).

116. Seok, H.-Y. *et al.* AtC3H17, a non-tandem CCCH zinc finger protein, functions as a nuclear transcriptional activator and has pleiotropic effects on vegetative development, flowering and seed development in *Arabidopsis*. *Plant Cell Physiol.* **57**, 603–615 (2016).
117. Rajkumar, R., Manikandan, A. & Saravanakumar, S. S. Physicochemical properties of alkali-treated new cellulosic fiber from cotton shell. *Int. J. Polym. Anal. Charact.* **21**, 359–364 (2016).
118. Amutha, V. & Senthilkumar, B. Physical, chemical, thermal, and surface morphological properties of the bark fiber extracted from *Acacia concinna* plant. *J. Nat. Fibers* **18**, 1661–1674 (2021).
119. Westman, M. P., Fifield, L. S., Simmons, K. L., Laddha, S. & Kafentzis, T. A. *Natural Fiber Composites: A Review* (2010).
120. Reddy, K. O., Maheswari, C. U., Reddy, D. J. P. & Rajulu, A. V. Thermal properties of Napier grass fibers. *Mater. Lett.* **63**, 2390–2392 (2009).
121. Jones, D., Ormondroyd, G. O., Curling, S. F., Centre, B. & Kingdom, U. *Chemical Compositions of Natural Fibres* (Elsevier, 2017).
122. Yussuf, A., Massoumi, I. & Hassan, A. Comparison of polylactic acid/kenaf and polylactic acid/rise husk composites: The influence of the natural fibers on the mechanical, thermal and biodegradability properties. *J. Polym. Environ.* **18**, 422–429 (2010).
123. Bledzki, A. K., Mamun, A. A. & Volk, J. Physical, chemical and surface properties of wheat husk, rye husk and soft wood and their polypropylene composites. *Composites Part A* **41**, 480–488 (2010).
124. Sreekumar, P. A. *et al.* Transport properties of polyester composite reinforced with treated sisal fibers. *J. Reinf. Plast. Compos.* **31**, 117–127 (2012).
125. Milanese, A. C., Cioffi, M. O. H. & Voorwald, H. J. C. Thermal and mechanical behaviour of sisal/phenolic composites. *Compos. Part B Eng.* **43**, 2843–2850 (2012).
126. Faruk, O., Bledzki, A. K., Fink, H. P. & Sain, M. Biocomposites reinforced with natural fibers: 2000–2010. *Prog. Polym. Sci.* **37**, 1552–1596 (2012).
127. Soatthyanon, N., Crosky, A. & Heitzmann, M. T. Comparison of experimental and calculated tensile properties of flax fibres. *J. Compos. Sci.* **6**, 100 (2022).
128. Mohajerani, A. *et al.* Amazing types, properties, and applications of fibres in construction materials. *Materials* **12**, 2513 (2019).
129. Arthanarieswaran, V. P., Kumaravel, A. & Saravanakumar, S. S. Characterization of new natural cellulosic fiber from *Acacia leucophloea* bark. *Int. J. Polym. Anal. Charact.* **20**, 367–376 (2015).
130. Manimaran, P., Saravanan, S. P. & Prithiviraj, M. Investigation of physico chemical properties and characterization of new natural cellulosic fibers from the bark of *Ficus racemosa*. *J. Nat. Fibers* **18**, 274–284 (2021).
131. Sanjay, M. R., Arpitha, G. R. & Yogesha, B. Study on mechanical properties of natural—glass fibre reinforced polymer hybrid composites: A review. *Mater. Today Proc.* **2**, 2959–2967 (2015).
132. Mohan, A. *et al.* Investigating the mechanical, thermal, and crystalline properties of raw and potassium hydroxide treated butea parviflora fibers for green polymer composites. *Polymers* **15**, 3522 (2023).
133. Hyness, N. R. J., Vignesh, N. J., Senthamaraiannan, P., Saravanakumar, S. S. & Sanjay, M. R. Characterization of new natural cellulosic fiber from heteropogon contortus plant. *J. Nat. Fibers* **15**, 146–153 (2018).

Acknowledgements

The authors gratefully appreciate the support given by K.R.Jaya Sheeba (Reg No: 19233042132010), Research scholar, PG & Research Department of Physics, Holy Cross College (Autonomous), Nagercoil – 629004, Affiliated to Manonmanium Sundaranar University, Tirunelveli, Tamil Nadu, India. The author thanks Vicerrectoria de Investigacion y Desarrollo (VRID) y Direccion de Investigacion y Creacion Artistica DICA, Proyecto presentado al Concurso VRID-Iniciación 2022, VRID N°2022000449-INI, Universidad de Concepción, Concepción, Chile. Centro Nacional de Excelencia para la Industria de la Madera (ANID BASAL FB210015 CENAMAD), Pontificia Universidad Católica de Chile, Vicuña Mackenna 7860, Santiago, Chile.

Author contributions

K.R.J.S.—Conceptualization, Data curation, Formal analysis, Methodology, Project administration, Software, Validation, Writing—original draft. R.K.P.—Conceptualization, Formal analysis, Methodology, Project administration, Supervision, Validation, Visualization, Writing—review & editing. K.P.A.—Conceptualization, Formal analysis; Validation, Project administration, Visualization, Writing—review & editing. S.S.—Formal analysis, Methodology, Validation, Visualization, Writing—review & editing. S.A.—Methodology, Project administration, Supervision, Funding acquisition, Validation, Visualization, Writing—review & editing. E.S.F.—Project administration, Supervision, Funding acquisition, Validation, Visualization, Writing—review & editing.

Funding

The financial support from Universidad de Santiago de Chile, Usach, through project N°092218SF_POSTDOC, Dirección de Investigación Científica y Tecnológica, Dicyt. E.I.S.F. acknowledges funding coming from the Chilean National Research and Development Agency, ANID, research project Fondecyt Regular 1211767.

Competing interests

The authors declare no competing interests.

Additional information

Correspondence and requests for materials should be addressed to R.K.P. or S.A.

Reprints and permissions information is available at www.nature.com/reprints.

Publisher's note Springer Nature remains neutral with regard to jurisdictional claims in published maps and institutional affiliations.



Open Access This article is licensed under a Creative Commons Attribution 4.0 International License, which permits use, sharing, adaptation, distribution and reproduction in any medium or format, as long as you give appropriate credit to the original author(s) and the source, provide a link to the Creative Commons licence, and indicate if changes were made. The images or other third party material in this article are included in the article's Creative Commons licence, unless indicated otherwise in a credit line to the material. If material is not included in the article's Creative Commons licence and your intended use is not permitted by statutory regulation or exceeds the permitted use, you will need to obtain permission directly from the copyright holder. To view a copy of this licence, visit <http://creativecommons.org/licenses/by/4.0/>.

© The Author(s) 2023